Chapter 2

Perfect metamaterial absorber in the visible region

In this chapter, we have discussed the polarization-insensitive-based metamaterial absorber structures consisting of three layers of metal-dielectric-metal. In the structure, a gallium arsenide material is taken with aluminum metal. This structure exhibits wideband, wide-angle, and polarization-independent absorption performance in the visible region due to matching the impedance of metamaterial with free space impedance. Under a specific condition, this simulated absorber structure exhibits an extremely broadband absorption in the applied wavelength range with near-unity absorption. Moreover, the parametric study of the design of metamaterial structures has also been investigated. The polarization-insensitive-based metamaterial may be utilized to improve the efficiency of different devices in the visible range.

2.1 Introduction

The first chapter discusses the characteristics of metamaterials and their flawless absorption of solar energy. After that, the methodologies for creating and analyzing as well as the techniques for validation are discussed. This chapter briefly introduces metamaterial absorber designs that have the potential to harness solar light incidents on Earth. Herein, different classes of metamaterial absorbers for solar energy harvesting are presented. Section 2.2 demonstrates a design of metamaterial structure for photovoltaic applications. The proposed absorber models are illustrated in section 2.2, in section 2.3 the metamaterial shows double negative properties and polarization independence for the visible light spectrum.

Utilizing solar radiations mainly in the visible region requires the perfect absorption of light for many energy fields including sensor[108], thermophotovoltaic[109], and solar cells[110]. In recent years, metamaterials have attracted considerable attraction because they are dramatically manipulating and absorbing incident electromagnetic waves[68]. The exotic and exciting optical properties of the metamaterial have motivated researchers to focus on the different applications using such materials. Metamaterials are artificial materials with a sub-wavelength metal-dielectric structure. The physical properties like effective permittivity $\varepsilon(\omega)$, permeability $\mu(\omega)$, and refractive index (n) of these materials are assumed negative values[6,111]. Metamaterials have been used across various frequency regions such as gigahertz, terahertz, and optical for many purposes such as antenna[112], detector[113], sensors[27,114], energy harvesting[115], and perfect absorbers[116,117]. Perfect absorption of a specific range of electromagnetic (EM) radiation is a very important property of the metamaterials for applications such as micro-bolometers[118], sensors[28], imaging[119], and solar energy harvesting[120,121]. Perfect absorption can be realized when the frequency-dependent effective impedance of the metamaterial absorber becomes the same as the impedance of

free space so that the reflected and transmitted waves reduce to zero[122]. These properties are utilized to obtain electrical energy from electromagnetic energy in thermo-photovoltaic devices such as absorbers[123], emitter[93], photodetectors[124], etc. It has also been observed that solar radiation can be captured by the metamaterial to improve the efficiency of photovoltaic devices. Mostly the energy of solar radiation[46] covers ranges between 390 nm to 700 nm. Therefore, we need a high absorption in the range of 390 nm to 700 nm solar radiation for efficient solar cells, which can be easily achieved by a suitable metamaterial absorber. Ultra-thin broadband super-absorbers have also been theoretically and experimentally proposed for different applications[125,126].

The first metamaterial[68] perfect absorber was proposed in 2008. This metamaterial structure consists of two plates of metal and a ring resonator with supplies the electric coupling. Most of the researchers have focused on a terahertz frequency region. Recently, reported metamaterial perfect absorber designs have provided the single-band[127,128], dual-band[129], and multi-band[130] absorbers to improve energy harvesting in the solar cell[123,131]. In the high-frequency region, multi-band metamaterial absorbers mainly provide the perfect absorption by using multiple layers. Some researchers[120,132] have reported the metamaterial absorbers, which consist of three layers in the form of metal-dielectric-metal. They have reported multiple absorption bands in the visible and infrared regions for different unit cell structure engineering. Different metamaterial absorbers have been presented for solar energy harvesting using simplified and compact structures with highly efficient broadband, polarization-independent, and wide-angle absorptions. The published papers[133,134] have demonstrated the broadband visible metamaterial absorbers with a compact and low-profile design for emitter and energy harvesting applications. Nevertheless, metamaterial perfect absorber structural engineering still needs to optimize

and simplify to undertake electromagnetic energy harvesting by developing more efficient absorbers.

Solar energy is the most abundant and cleanest renewable energy source that can be captured and converted into thermal and electrical energy. Earth's surface gets a different amount of energy for different types of radiations and incident angles[135]. Visible radiations are playing a crucial role in solar cell applications and offer a maximum current in output. The conversion efficiency is reduced by any loss of light for solar cells. Its loss can be reduced by tiny transmission from the bottom metallic layer and minimum reflection with the help of metallic metasurface which improved the performance of solar cells. Some researchers carefully designed the absorbers to absorb some photons of visible regions with costly metals and had a low absorption efficiency (71%) that not be useful for solar cell applications[136]. Besides these features, the short circuit current density (J_{sc}) is the actual property to investigate the solar cell device. We required the high J_{sc} for potential applications with cheaper metals to reduce the cost of the device[137].

In this chapter, we have introduced a new design of metamaterial absorber for highly efficient solar energy absorption. The proposed absorber is composed of a metal-dielectric-metal nanostructure. The proposed absorber provides nearly perfect absorption in the visible region from wavelengths 375 nm to 750 nm using aluminum metal resonators on the gallium arsenide dielectric spacer layer and represents the 80.74% average absorption. The characteristics of the absorber have been investigated for different geometric parameters of the structures and resonators and spacer materials. Moreover, we have also investigated the effect of polarization and incident angles on the absorptions of the proposed structure. The conversion efficiency was significantly improved by the large value of $A_{AM1.5}$ under the AM1.5 solar spectrum of the solar cell. We obtained the short

circuit density under the AM1.5 solar illuminations and it has great potential for solar cell applications.

2.2 Design and Simulation

2.2.1 Geometry and Materials

The proposed absorber structure is composed of three basic layers such as a bottom metallic layer of thickness '*h*', a dielectric spacer layer of thickness '*t*', and metallic patch resonators of thickness 'h_1'. The proposed design and geometric parameters of the metamaterial absorber are shown in Fig. 2.1, and the value of each parameter is tabulated in Table 2.1. The periodicity of the unit cell *'p'* is liable for the resonance condition at different frequencies. The structure has two parts of metal layers which are Al (Aluminium) as the resonators and GaAs (Gallium arsenide) as a dielectric spacer layer. We have selected aluminum metal because it is inexpensive and has less production cost as compared to the other metals (gold, silver, and copper) for the design of different types of metamaterial absorber structures[138]. In several published papers[130,133,135,139], the researchers have utilized Al metal to design the different metamaterial absorber structures and investigated their behaviors in the ultra-violet, visible, and near-infrared regions, respectively.

2.2.2 Simulation software and boundary conditions

We have used CST microwave studio simulation software to simulate the proposed metamaterial absorber structure. The software has adopted the aluminum (Al) parameter values of electric conductivity $\sigma = 3.56 \times 10^7 \mathrm{S/m}$, Rho ($\rho$) = 2700 $\mathrm{kg/m^3}$, thermal conductivity (K) = 237 [W/K/m] in the range 150 THz- 2900 THz. These parameters are in good agreement with the aluminum parameters of previously reported papers[138,140,141]. We have considered the range of the proposed absorber from 375 nm to 750 nm. In the proposed structure, we have considered the bottom layer to be a metallic aluminum plate with a thickness greater than its skin depth for the operating frequency to eliminate

transmission losses. The semiconductor material of GaAs has some vital advantages such as high efficiency, high electron mobility and velocity, low-temperature coefficient, low light performance, and flexibility, etc. It has a direct bandgap that forms a good solar energy absorber. The description of GaAs[140,141] are $\varepsilon = 12.94$, loss tangent (tanδ) = 0.006, ρ = 5320 [kg/m^3] and the thermal conductivity (K) = 54 [W/K/m].

To gain an efficient absorption level from scattering parameters, we applied the periodic boundary conditions for the proposed metamaterial structure. The unit cell periodic boundary conditions (PBCs) have been applied to the x and y-plane and the open-source was set in the z-direction (Floquet port) with a Perfectly matched layer, respectively. All the axis are perpendicular to each other in the simulation setup[130].

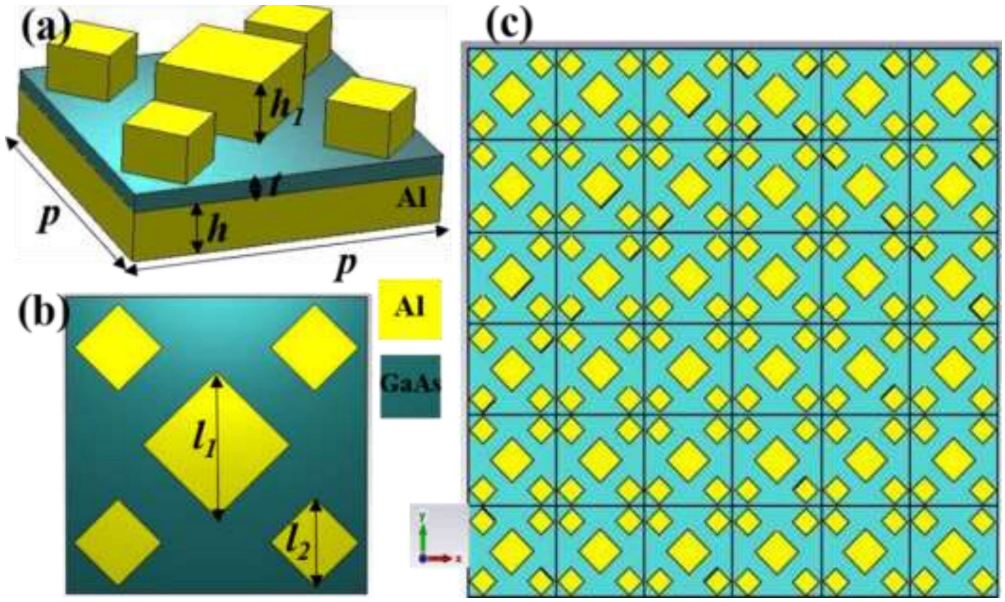

Fig. 2.1 (a) Schematic diagram of the metamaterial absorber, **(b)** program view, **(c)** perspective view of a unit cell with the periodic range.

Table 2.1 Respective parameter (nm) of the proposed metamaterial absorber.

Parameter	***p***	***h***	***t***	h_1	l_1	l_2
Value (nm)	610	100	37	100	150	90

2.2.3 Methodology and absorbance of the proposed unit cell

In this work, we have chosen the CST microwave studio software for the simulation of the proposed structures. This software is a full-wave electromagnetic solver that uses the well-known theory FIT (Finite Integration Technique) to calculate the optical properties of the structures. So we have presented the absorption expression directly based on the scattering parameters. These scattering parameters can be used to evaluate the absorption[133,141]. The reflectance R(ω) and transmittance T(ω) depend on the scattering parameters such as R(ω) = $|S_{11}|^2$ and T(ω) = $|S_{21}|^2$. The scattering parameters S_{11} and S_{21} are described as

$$S_{11} = \sqrt{\frac{Reflected\ power\ form\ port1}{Incident\ power\ from\ port1}} \tag{2.1}$$

$$S_{21} = \sqrt{\frac{Transmitted\ power\ form\ port2}{Incident\ power\ from\ port1}} \tag{2.2}$$

The optical absorption properties of the proposed metamaterial absorber in terms of frequency can be calculated by using the well-known equation expressed as,

$$A(\omega) = 1 - R(\omega) - T(\omega) \tag{2.3}$$

Where A(ω) and ω represent the absorption and angular frequency, respectively. In the proposed metamaterial structure, the thickness of the bottom aluminum layer is considered more than the skin depth, so it works as a reflector in the optical region so that the transmitted waves cannot pass through the structure. The absorber system contains two

interfaces. One is the resonator layer, and the other is the ground film of Al metal. These layers act as a reflection/transmission surface that can reflect/transmit a part of the incident wave. If the considered ground layer works as a perfect reflector, the transmission will be approximately zero. Therefore, transmission becomes approximately zero in the above equation. Therefore, Eq. 2.3 can be written as;

$$A(\omega) = 1 - R(\omega) = 1 - |S_{11}|^2 \quad (2.4)$$

In the metamaterial structure, the periodic arrangement of the resonator at the top of the dielectric substrate plays a crucial role to gain a perfect absorber. Scattering parameters (S-parameter) are used for the absorption calculation of the proposed absorber. The condition of impedance matching is necessary to gain absorption because absorption depends on the impedance. The impedance of the proposed structure unit cell can be optimized by matching the impedance of metamaterial with free space impedance. By investigating the physical dimensions of the structure, the conditions of impedance matched with free space and the design structure give the near-unity absorption at an operating wavelength. Here, the impedance of the design is very close to the impedance of free space, if these values are equal then the design absorber act as a super absorber.

2.3. Results and discussion

2.3.1 Charsterstics of absorbance

Solar radiation covers the near-infrared to ultraviolet (100 to 1000 THz) frequency region but our work is in the visible region because it is widely used for various applications. To observe the optical performance of the proposed structure, we have used Eq. 2.4 to calculate the absorption and reflection of the absorber as shown in Fig. 2.2. Fig. 2.2(a) manifested the absorption characteristics for the metamaterial absorber with Al metal as the resonators and GaAs as a dielectric spacer layer. This design exhibits excellent broadband absorption in the optical region. We observe approx 99.99% broadband

absorption from 591.54 nm to 704.40 nm (112.86 nm bandwidth) and an almost unity peak at 385.33 nm with 94.16%. In the broadband absorption region, we observe the three highest absorption peaks. These absorption peaks have 99.82%, 99.94%, and 99.94 % absorption coefficients for the different wavelengths as 603.44 nm, 651.72 nm, and 692.05 nm, respectively. The comparison of the proposed metamaterial absorber with the literature work is presented in Table 2.2. When the electromagnetic wave strikes the absorber, some of the incident light is reflected in the free space which a coefficient is S_{11} while some of the incident light is transmitted by region 1 to region 2 which a coefficient is S_{21}. Here S_{11} and S_{21} represent the reflection and transmission coefficients, respectively. Fig. 2.2(b) exhibits the real and imaginary parts of impedance. Here transmittance power is zero ($|S_{21}| = 0$) because the bottom layer of Al can not pass the light due to skin depth. We observe that the real and imaginary impedances at the unity absorption wavelength (385.33 nm, 603.44 nm, and 692.05) are close to near unity and zero, respectively. The effective impedance of the absorber is calculated by the scattering coefficients using the standard equation[6],

$$Zeff = \sqrt{\frac{(1 + S_{11})^2 - S_{21}^2}{(1 - S_{11})^2 - S_{21}^2}} = \frac{1 + S_{11}}{1 - S_{11}} \tag{2.5}$$

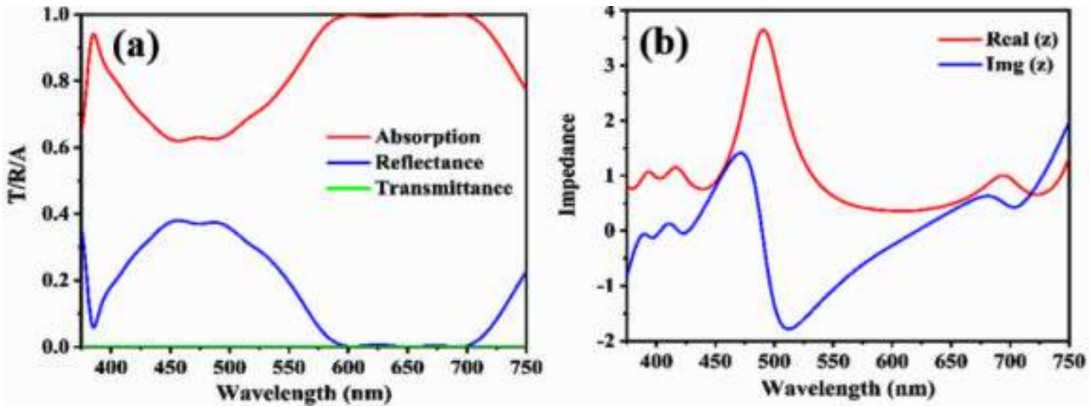

Fig. 2.2 (a) Absorption, Reflectance, and transmittance spectra, **(b)** the real and imaginary impedance of the proposed structure.

2.3.2 Effective values of permittivity and permeability

The constitutive electromagnetic parameters such as effective permeability (μ_{eff}) and permittivity (ε_{eff}) can be calculated by the co-polarized reflection coefficient. The magnetic susceptibility (χ_{ms}) and electric susceptibility (χ_{es}) help to evaluate (μ_{eff}) and (ε_{eff}) with distance (d) to be traveled by propagating wave, where $k_0 = 2\pi f/c$ is the wavenumber of the free space. We observe the negative values for the real part of permittivity and permeability within some specific wavelength regions from the results as shown in Fig. 2.3. The variations of the real and imaginary parts of the effective permeability (μ_{eff}) and permittivity (ε_{eff}) are shown in Fig. 2.3. The expressions of the electric susceptibility (χ_{es}), magnetic susceptibility (χ_{ms}), effective permittivity (ε_{eff}) and permeability (μ_{eff}) are given below as[142143],

$$\chi_{es} = 2j/k_0*(1-S_{11}/1+S_{11}) \quad (2.6)$$

$$\varepsilon_{eff} = 1 + \chi_{es}/d \quad (2.7)$$

$$\chi_{ms} = 2j/k_0*(1+S_{11}/1-S_{11}) \quad (2.8)$$

$$\mu_{eff} = 1 + \chi_{ms}/d \quad (2.9)$$

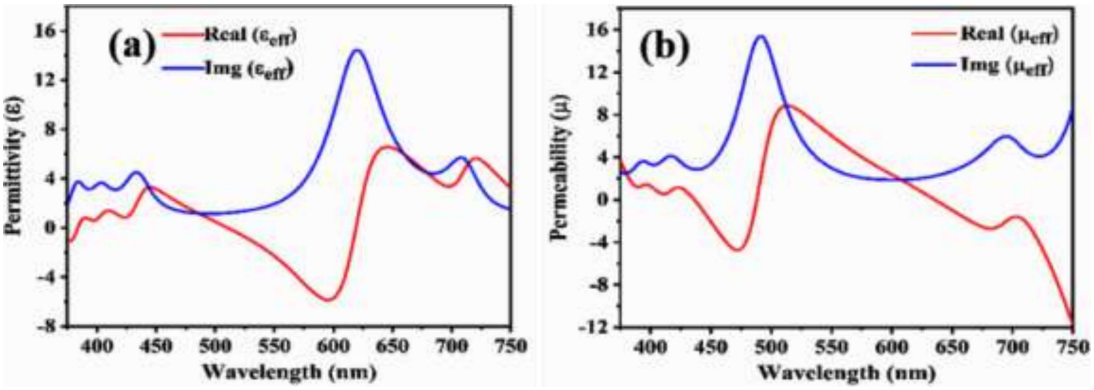

Fig. 2.3 The variations of the real and imaginary parts of the effective **(a)** permittivity, **(b)** permeability.

2.3.3 Effect of resonators on absorbance

To demonstrate the absorption responses for different cases, we have demonstrated the absorption, transmission, and reflection responses for Al substrate only, substrate Al-GaAs layer, and substrate Al-GaAs-Al resonators system in Fig. 2.4. We observe the maximum reflection, zero transmission, and approximately 8% average light absorption from the Al substrate as design (a). The absorption response exhibits around 45% absorbance for the structure of the Al-GaAs layer, as seen in design (b). These results are due to the interaction between the absorbing and bottom layers. Maximum absorption is approximately 68.55% at the wavelength of 553.12 nm. When the inner resonator is established at the center of the dielectric spacer layer as design (c), the interaction of the resonator with the dielectric spacer layer and the bottom layer is formed three absorption peaks, as can be seen in the diagram. We obtain a perfect absorption of more than 99% absorption value at the resonance wavelengths 387.13 nm, 419.41 nm, and 607.35 nm. The response for the structure with corner resonators as design (d) is marked as a bold blue curve which gives a broader absorption response compared to the previous absorption level. This response gives the interaction between the corner resonator pairs and the other part of the structure with the help of electromagnetic responses. Finally, we have depicted the absorption responses for the combined resonators in one unit cell as design (e) in Fig. 2.4 with a bold red curve. The interactions between the resonator and the coupling of Al-GaAs create plasmonic effects, which are responsible for increasing the strength of the absorption. These results reveal the multiband topology for different structural arrangements. The significant absorption is the result of stimulated absorption in material GaAs due to Al material as a resonator and substrate layer with maximum reflection. The uses of Al materials as the resonators and reflector layer only trigger the efficient absorption in absorbing material because Al materials have a minimal absorption value. This result is due to the coupling of

reflection and transmission and the plasmonic resonance effects of resonators and reflector layer.

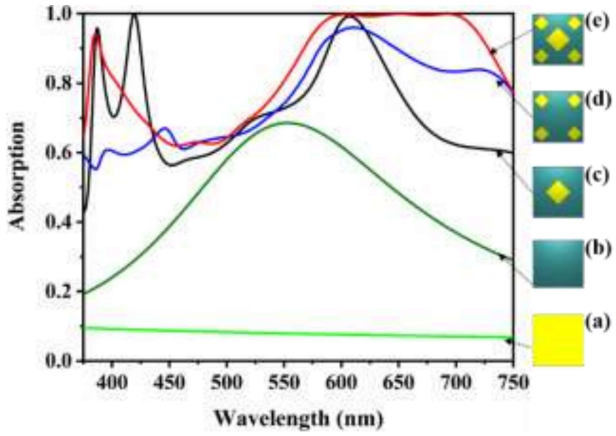

Fig. 2.4 Absorption variations with frequency for the structure with **(a)** Al substrate only, **(b)** Al-GaAs system, **(c)** with only center resonator, **(d)** with corner resonators, **(e)** with corner and center resonators (complete unit cell).

2.3.4 Absorbance performance on period and thickness of the dielectric layer

To understand the absorption characteristics, it is necessary to know the impact of the geometric parameters. For the absorption mechanism, the parameters of dielectric layer thickness t, resonator diagonal lengths l_1, and l_2, and the structural periodicity p perform a very important role in the variation of absorption spectra. Firstly, we examine the effect of the dielectric layer thickness represented by the parameter t. The thickness of the dielectric layer can modulate the resonant wavelength and rate of absorption as shown in Fig. 2.5(a). It mainly helps the coupling between the resonators and the ground aluminum layer. Therefore, the magnetic response is generated by this coupling. Thus, the impedance matching of the absorber with the free space impedance verifies the electric and magnetic distribution. So, the thickness of dielectric separation generates the magnetic response when the parameter 't' is smaller and higher than 37 nm. The impedance condition does not match other thicknesses (t), so absorption spectra are changed. Therefore, thickness plays a crucial role in the considered design absorber. The variations of the absorption with

the periodicity of the unit cell '*p*' are shown in Fig. 2.5(b). When the period of a unit cell increases, the resonance peaks shift toward a higher wavelength with changed absorption values. It originates from the resonators because Electric-field and Magnetic-field are changing their positions. Therefore, we observe that the maximum absorptions are affected by changes in the periodicity and the optimized value is p = 610 nm to obtain the perfect absorption.

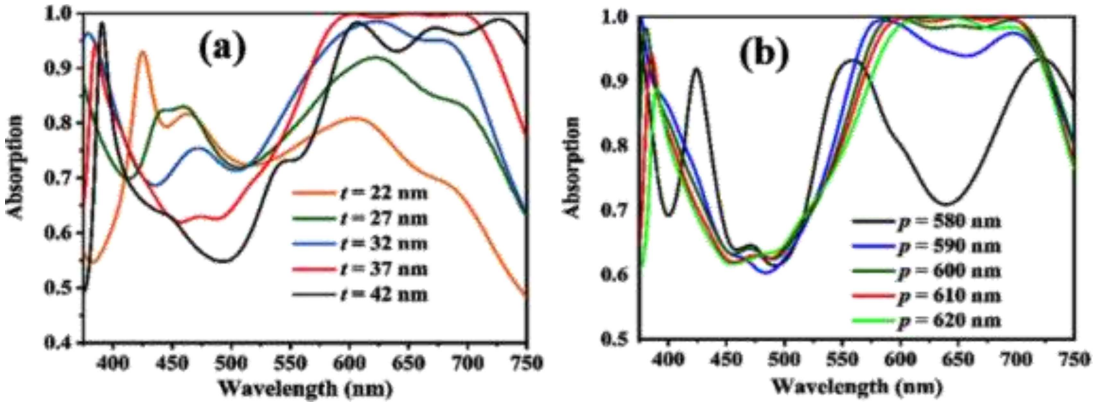

Fig. 2.5 Absorption spectra for different values of **(a)** dielectric layers thickness *'t'*, **(b)** periodicity parameter *'p'*.

2.3.5 Absorbance performance on the thickness and diagonal length of resonators

In the design of the absorber, the resonator's dimension selection also plays an important role in investigating the perfect absorption. Tuning the resonator's dimension influences the absorption spectrum with constant values of the other parameters. The results with different resonator dimensions are shown in Fig. 2.6. The red curve represents the desired results for perfect absorption. As seen in Fig. 2.6(a), the absorption depends on the diagonal length of resonators so this section explained the optimization of the diagonal length l_1 of the middle resonator. The variations of the absorption with the diagonal length of the middle resonators are shown in Fig. 2.6(b). The resonance wavelength 591.54 to 704.40 nm and 385.33 nm are strongly dependent on the diagonal length of resonators which give the transformation of electric and magnetic responses at this wavelength. This result is the interaction between

resonators. Therefore, finding the perfect absorption requires adjusting the diagonal length 'l_1'. Similarly, we have investigated the absorption results with a different diagonal length of corner resonators at the same wavelength. The distributions of the absorption at the different values of diagonal length 'l_2' are shown in Fig. 2.6(b). We obtain the best results with diagonal length l_2 = 90 nm as seen in Fig. 2.6(b). Thus, the properties of the metamaterial absorber can be modulated by adjusting the individual resonators or their grouping.

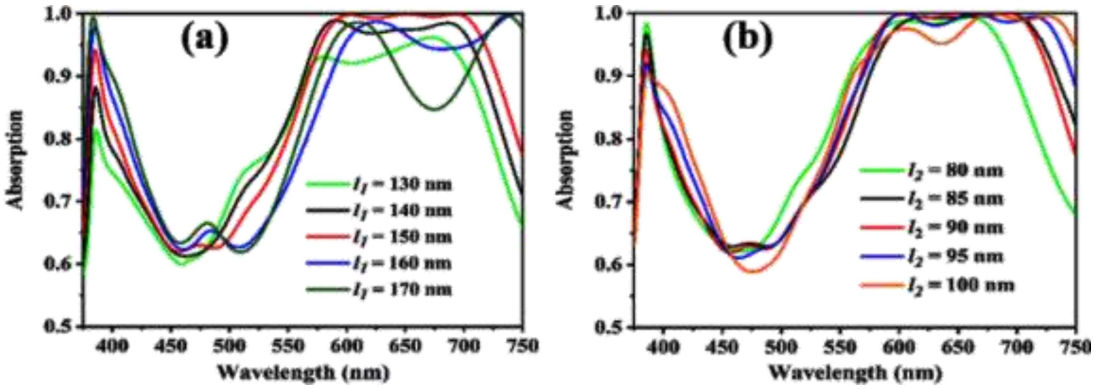

Fig. 2.6 Absorption spectra for various values of **(a)** the diagonal length *'l_1'* of the middle resonator, **(b)** the diagonal length *'l_2'* of the corner resonator.

2.3.6 Absorbance performance on polarization and incidence angles

The directions of the solar radiation change every time in the sky and some parts of the incident radiation on the unit cell are in the form of unpolarised radiations. Thus, a convenient metamaterial unit cell design is required to operate for all the incident electromagnetic radiations for optimizing the absorption. The simulated absorption results for both modes at different polarisation angles are shown in Fig. 2.7(a) and 2.7(b). It can be seen that the absorption spectra for different polarization angles (0°-90°) are the same within the operating wavelength because the proposed design is symmetrical. In the visible region, the polarization angle is very important for the design of a metamaterial absorber because efficient absorption is necessary for solar cells. The absorption spectra with various incident angles (θ) are shown in Fig. 2.7(c) and 2.7(d) to characterize the absorber

performance at different incident angles (0°-50°) for TE and TM-modes. The absorption coefficients decrease with increasing the incident angles for TE mode as shown in Fig. 2.7(c). The distributions of absorption with incident angle are mainly affecting within the wavelength range 591.54 nm to 704.40 nm due to the electric and magnetic mode excitations. Fig. 2.7(d) shows the absorption spectra for TM mode. In this case, we obtain the broadband absorption efficiency as compared to the TE mode's absorption, and absorbance increases with the incident angles. The comparison of our results with the previously reported papers is tabulated in Table 2.2. The proposed absorber exhibits a good absorption level compared to the previously reported works in terms of their absorption coefficients, impedance, and production cost.

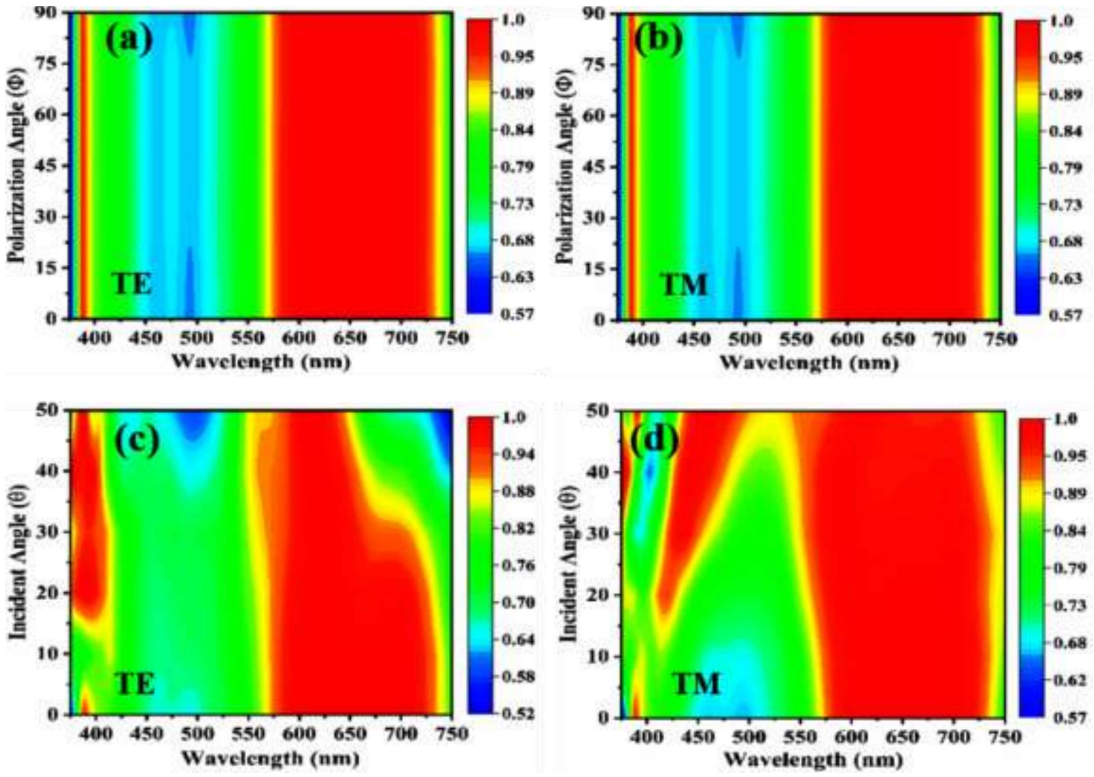

Fig. 2.7 (a, b) Absorption spectra for the different polarization angles (0°-90°), **(c, d)** the different incident angles (0°-50°) with TE mode and mode.

Table 2.2 Comparative study of the proposed metamaterial absorber with previously reported research papers.

Reference	Dimensions of a unit cell	Dielectric thickness (nm)	Functionality	Absorptivity (%)
128	550 x 550	100 nm	Single band	99.7 %
129	600 x 600	93.5 nm	Dual-band	99.96 % 99.37 %
130	400 x 400	50 nm	Multiband	99.2%, 99.8%, 99.9%
135	400 x 300	80 nm	Multiband	Above 90 %
144	580 x 580	111.6 nm	Multiband	99.95%
145	1000 x 1000	100 nm	Multiband	99.9%
This work	610 x 610	37 nm	Wideband	>99 %, 94.16%

2.3.7 Absorbance comparison with various metals and dielectric layers

Nowadays, different materials are used for different layers to gain strong absorption. So, We have used different metals (Au, Ag, Cu, and Al) for resonators to investigate the performance of our proposed design absorber. Fig. 2.8(a) shows the simulated absorption results with different resonator metals. As a result, we obtain the perfect absorption for the proposed absorber with Al over the whole optical region as can be seen in Fig. 2.8(a). The selections of the resonator metals are very important because it reveals the coupling of surface plasmons which helps to achieve strong absorption. Fig. 2.8(b) demonstrated the absorption performance with various materials (silicon dioxide (SiO_2), silicon nitride (Si_3N_4), indium tin oxide (ITO), and gallium arsenide (GaAs)) of the dielectric spacer layers. The absorption changed with different bandwidths for each of the spacer materials, and GaAs show the strong and highest absorption coefficients as compared to other dielectric materials.

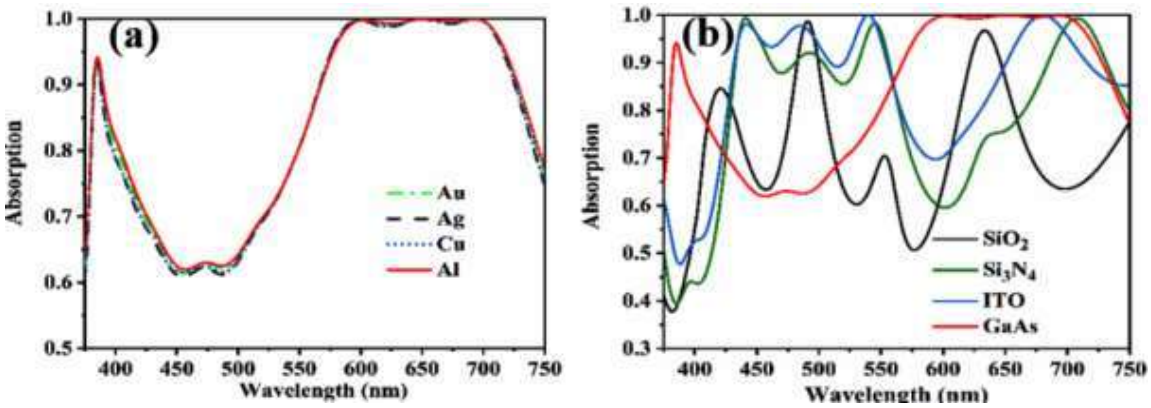

Fig. 2.8 Absorption spectra for **(a)** the different resonator metals such as Au Ag, Cu, and Al, **(b)** the dielectric spacer layer of SiO_2, Si_3N_4, ITO, and GaAs.

2.3.8 Conversion efficiency performance on dielectric layer and periodicity

Various parameters of structure demonstrated different absorbances in the optical region. Here we evaluated the absorbance under the AM1.5(air mass 1.5) solar spectrum ($A_{AM1.5}$) of the solar cell. A large conversion efficiency can be obtained when the value of $A_{AM1.5}$ is higher. To check the light trapping effect[143] the unit cell used the $A_{AM1.5}$. In this context, the proposed absorber provides ultra-wideband absorption in the optical spectrum.

From this expression, we can obtain the $A_{AM1.5}$ of the solar cell,

$$A_{AM1.5} = \frac{\int_{\lambda 1}^{\lambda 2} A(\lambda)N(\lambda)d\lambda}{\int_{\lambda 1}^{\lambda 2} N(\lambda)d\lambda} \tag{2.10}$$

Where, λ is the wavelength of light, λ_1, and λ_2 define the spectrum range of absorption, Thickness (λ) is the absorption of investigated structure, and $N(\lambda) = \frac{w(\lambda)}{E(\lambda)}$ is the photon numbers distribution under the AM1.5 solar illumination. Where w(λ) and E(λ) represents the solar spectral irradiance and energy of the photon. We evaluated the A(λ) and N(λ) using with below equation under the different geometrical parameters of structure as the dielectric thickness (*t*) and the dimension of the unit cell (*p*). Fig. 2.9(a) and 2.9(b) shown the maximum $A_{AM1.5}$ is 85.78% for t = 37 nm and 86.12% for p = 600 nm. The value of conversion efficiency (representing $A_{AM1.5}$) of solar cells should be maximum.

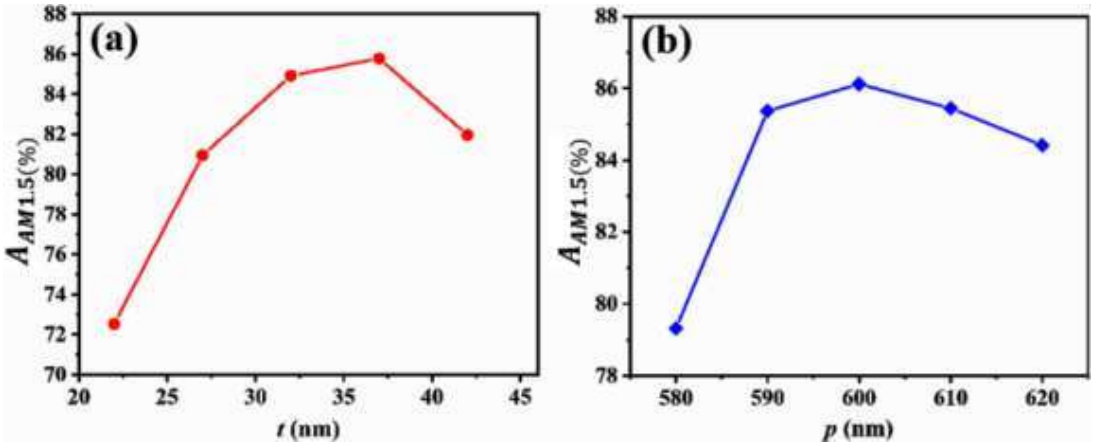

Fig. 2.9 The evaluated values of $A_{AM1.5}$ as a function of **(a)** dielectric thickness (t), **(b)** unit cell dimension (p).

2.3.9 Short circuit current density and solar spectrum

This type of metamaterial absorber can be used for solar energy harvesting applications. Therefore, in this section, we will try to evaluate the value of short circuit current density (J_{sc}) for photovoltaic devices. Fig. 2.10(a), demonstrated J_{sc} with the different thickness effects of the dielectric layer of GaAs. One electron-hole pair is generated by each absorbed photon and collected carriers are generated by all photons. J_{sc} under AM1.5 solar irradiance can be calculated by this expression[146],

$$J_{sc} = \frac{q}{hc}\int_{\lambda 1}^{\lambda 2} \lambda\, \Phi_{AM1.5}\, A(\lambda) d\lambda \tag{2.11}$$

Here, q is the charge of an electron, λ is the wavelength of the incident light, c is the speed of light, h is the Plank constant, A(λ) is the absorption of this absorber, $\Phi_{AM1.5}$ is the solar radiance, and considering the quantum efficiency (internal) is 100%. When the GaAs thickness is tuned from 22 nm to 42 nm with an interval of 5 nm, J_{sc} is not regular because J_{sc} mainly depends on the number of resonant modes generated in the 375-750 nm wavelength range as shown in Table 2.3. The maximum J_{sc} obtained for t = 32 nm, which is 20.10 mA/cm^2, for t = 37 nm, J_{sc} = 20.33 mA/cm^2, which is greater than the J_{sc} of 17.08 mA/cm^2, 13.2mA/cm^2, 14.09mA/cm^2 reported paper[137,147,148]. From the response of solar

absorption, can find the solar energy collection. The ideal absorber has >99% absorbance in the operating region and shows a wide bandwidth. We investigated the solar absorption of the proposed absorber under the irradiance of the AM1.5 source. In Fig. 2.10(b), somewhere energy is missed, but somewhere energy is matched under the illumination there efficiency is high of capture light. Therefore, this absorber can be used the solar cell and solar energy harvesting-related potential applications.

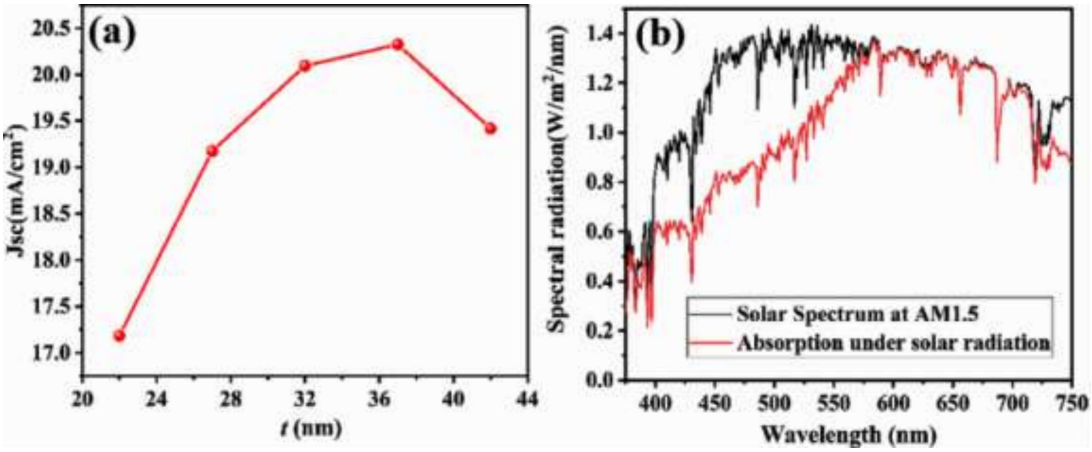

Fig. 2.10 (a) Short circuit current density (J_{sc}) with various thicknesses of GaAs layer, **(b)** absorption diagram of absorber under the AM1.5 solar spectrum.

Table 2.3 J_{sc} with different thicknesses (t) of a dielectric layer.

Thickness (t)	**22 nm**	**27 nm**	**32 nm**	**37 nm**	**42 nm**
J_{sc}**(mA/cm²)**	17.18	19.17	20.10	20.33	19.42

2.4 Conclusions

In this study, we have presented a polarization-insensitive-based metamaterial absorber structure that exhibited a near-unity absorption from 591.54 nm to 704.40 nm due to impedance-matching conditions. The proposed structure has been designed with three effective layers arrangement (metal-dielectric-metal). The position and amplitude of absorption bands can be tuned with the parameters of resonators and the thickness of the constituted dielectric layer. The effects of polarization angles and incident angles on the

absorption of the design have also been demonstrated. The large value of $A_{AM1.5}$ indicates improved conversion efficiency and promising for solar cell applications. This absorber can be applied in electricity because it has a high short circuit current density of over 20.33 mA/cm^2. Moreover, this kind of absorber can be used to design optical detectors, sensors, optical imaging, and solar energy harvesting devices.